

Porous NiTi shape memory alloys produced by SHS: microstructure and biocompatibility in comparison with Ti₂Ni and TiNi₃

Paola Bassani · Silvia Panseri · Andrea Ruffini ·
Monica Montesi · Martina Ghetti · Claudio Zanotti ·
Anna Tampieri · Ausonio Tuissi

Received: 22 January 2014 / Accepted: 3 June 2014 / Published online: 14 June 2014
© Springer Science+Business Media New York 2014

Abstract Shape memory alloys based on NiTi have found their main applications in manufacturing of new biomedical devices mainly in surgery tools, stents and orthopedics. Porous NiTi can exhibit an engineering elastic modulus comparable to that of cortical bone (12–17 GPa). This condition, combined with proper pore size, allows good osteointegration. Open cells porous NiTi was produced by self propagating high temperature synthesis (SHS), starting from Ni and Ti mixed powders. The main NiTi phase is formed during SHS together with other Ni–Ti compounds. The biocompatibility of such material was investigated by single culture experiment and ionic release on small specimen. In particular, NiTi and porous NiTi were evaluated together with elemental Ti and Ni reference metals and the two intermetallic TiNi₃, Ti₂Ni phases. This approach permitted to clearly identify the influence of secondary phases in porous NiTi materials and relation with Ni-ion release. The results indicated, apart the well-known high toxicity of Ni, also toxicity of TiNi₃, whilst phases with higher Ti content showed high biocompatibility. A slightly reduced biocompatibility of porous NiTi

was ascribed to combined effect of TiNi₃ presence and topography that requires higher effort for the cells to adapt to the surface.

1 Introduction

Nickel–titanium intermetallic alloys with a molar composition close to 1:1 are known as ‘shape memory alloys’ (SMA): they exhibit special thermo-mechanical properties known as shape memory effect and superelasticity. These properties are related to a thermoelastic, reversible, martensitic transformation between the austenite phase, stable at high temperature and a martensitic phase, stable at low temperature. The related phenomena are exhaustively illustrated in several reference works, consequently are not described in this paper [1, 2]. These peculiar functional properties of SMA promoted the development of several devices and components for medical applications, among which orthopedic implants, stents and surgery tools. One of the last applications is the use as bone substitution material: porous NiTi especially has been considered, as proper porosity of the material reduces apparent stiffness of the material giving mechanical properties close to those of cortical bone, and it can improve osteointegration at the surface [3–5].

For all biomedical applications biological compatibility is of utmost importance and hence many studies were performed in this field. A special concern was related to the high Ni content of the material: high released content of this metal leads to strong inflammation [6], and also at low concentration it could promote allergy. Positive results were generally reported for NiTi SMA that showed a behavior comparable to other biomaterial such as stainless steel and titanium alloys [7]. Most of the studies were

P. Bassani (✉) · A. Tuissi
Unit of Lecco, Institute for Energetics and Interphases, National
Research Council of Italy - IENI-CNR, Corso Promessi Sposi
29, 23900 Lecco, Italy
e-mail: paola.bassani@ieni.cnr.it

S. Panseri · A. Ruffini · M. Montesi · M. Ghetti · A. Tampieri
Institute of Science and Technology for Ceramics, National
Research Council of Italy - ISTECC-CNR, Via Granarolo 64,
48018 Faenza, Italy

C. Zanotti
Unit of Milano, Institute for Energetics and Interphases, National
Research Council of Italy - IENI-CNR, Via R. Cozzi 53,
20125 Milano, Italy

conducted on bulk NiTi materials, i.e. obtained from conventional melting of pure elements and subsequent metal working procedures, that generally result in a single phase microstructure. The concern about the influence of secondary phases was already envisioned, as they could deteriorate NiTi behavior especially in a severe environment [8–11]. The good biocompatibility of NiTi is generally ascribed to the oxidability of the material: after an initial release of Ni, a stable titanium oxide layer is rapidly formed at the surface that stops Ni release [12, 13]. Rondelli and Vicentini demonstrated that the repassivation ability of NiTi was lower than other alloys [14]. Shabalovskaya evidenced that strongly passivated NiTi has better behavior of mechanically polished NiTi with low secondary phases content, nevertheless the latter showed none or very low toxic effect [15]. The presence of secondary phases was generally discouraged in NiTi but few studies were devoted to this problem. Bogdanski et al. [8] performed an interesting work on functionally graded Ni–Ti samples. Their work evidenced the high toxicity of Ni, and of Ti–Ni alloys with high Ni content. Also alloys with TiNi₃ and Ti₂Ni intermetallic phases were considered, and a qualitatively worst behavior was observed for the first, while no appreciable difference with Ti and NiTi behavior was observed for the latter.

The presence of secondary phases can be of high concern especially for porous NiTi. This material can be produced by several routes, each characterized by various advantages and limitations. Two main production routes can be considered to obtain porous NiTi [5]: processing of prealloyed NiTi powders [3, 16], or reactive synthesis of elemental Ni and Ti powders. Among the latter group, self propagating high temperature synthesis (SHS) provides an ease, quick and energy saving method to obtain finished products. Mixed Ni and Ti powders are compacted in a pellets, rapidly heated in a protective atmosphere and ignited at one end: an exothermic reaction initiates and it self-propagates through the pellet and in few seconds the intermetallic NiTi compound is synthesized. Proper control of SHS process parameters, (such as preheating temperature, compaction degree, powder size...) can lead to NiTi samples of different porosity. Unfortunately a negative trend between porosity degree and phase composition is generally reported: single phase material is obtained at very high reaction temperatures, at which local melting of the pellet occurs and consequently pores collapse. On the other end, low reaction temperatures preserve pore structure at the expense of higher secondary phase content [17, 18].

Especially for porous NiTi hence the presence of secondary phases has to be monitored. Their influence on overall biological behavior of the material has to be considered. The threshold amount that induces toxic effect should be better defined, and differentiated according to

each secondary phase. In the present work we first report a comparison of the biological responses of bulk and porous NiTi, Ti₂Ni and TiNi₃ intermetallic compounds.

2 Materials and methods

2.1 Material preparation

Six materials were considered for the tests: porous NiTi, bulk NiTi, TiNi₃, Ti₂Ni, and pure Ni and Ti metals. Porous NiTi was produced by SHS starting from Ni and Ti powders (both <150 μm) mixed in equiatomic ratio (1/1). The powders were slightly compressed in pellets of 12 mm diameter and different heights (1–20 mm). Experimental set-up for SHS reaction is featured by a laser system (250 W) that is used to drive the volumetric sample heating and reaction ignition. Detailed description of SHS equipment was reported elsewhere [19]. Several samples were prepared with the same parameters. Porosity was evaluated through image analyses and weight to volume ratio on prismatic specimens. Values were in good agreement, leading to an average porosity of 45 %. Bulk NiTi was produced starting from commercially pure Ti (ASTM grade 1) and electrolytic nickel. The metals were vacuum induction melted and subsequently hot worked in order to obtain square section rolled bar of 5 × 5 mm² section. Ti₂Ni and TiNi₃ were produced through cold heart electric vacuum arc melting in the form of small ingots (about 20 × 10 × 180 mm³ in size). They were re-melted five times to assure good homogeneity. Finally, titanium (ASTM grade 1) and electrolytic nickel were also considered as pure metal references.

The specimens were cut from each raw material as square section prismatic samples with a metallographic diamond saw. Two sizes were considered: porous NiTi specimens were bigger (7.8 × 7.8 mm²) than all other specimens (7 × 7 mm²) in order to have a flat surface (about 60 % of the nominal surface, the remnant was pores) at least comparable to that of the other samples. In Fig. 1 representative samples of porous NiTi are shown, evidencing the engraved surface of the specimens. The sample thickness was adjusted in the range 0.5–3 mm on the basis of the mechanical properties of the material: Ti₂Ni and TiNi₃ specimens required higher thickness, due to the brittleness of these intermetallics. Accordingly the weight of each specimen varied from 200 to 1,100 mg (see Table 1). No specific heat treatment or passivation procedures were applied to the surface of the specimens that could mask material: only cleaning processes were applied, as explained in the following sections. Additional samples of proper size and surface finish (metallographic polishing through emery paper grinding followed by 6 and 1 μm

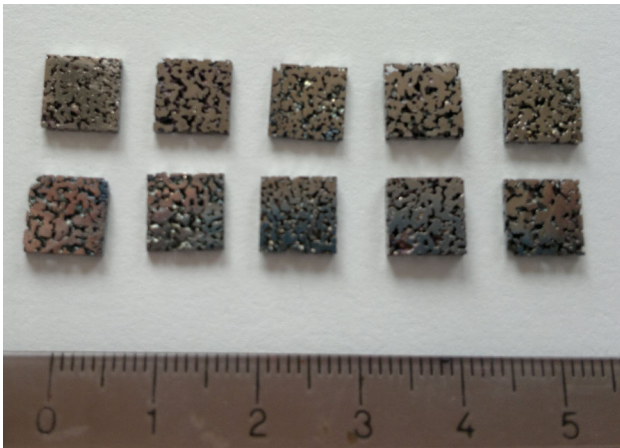


Fig. 1 Representative porous NiTi sample for biological tests

Table 1 Characteristics of the studied metallic samples

Sample	A	B	C	D	Bulk	Porous
Chemical formula	Ti ₂ Ni	TiNi ₃	Ti	Ni	NiTi	NiTi
Nickel content (wt%)	38.0	78.6	/	100	55.1	55.1
Average weight (mg)	818	1,110	109	653	292	206

diamond paste polishing) were prepared for microstructural investigation.

2.2 Material characterization tests

The microstructure of the samples was analyzed through a combination of X-ray diffraction and scanning electron microscopy (SEM). The X-ray diffraction patterns were recorded with θ/θ scans using a Philips PANalytical X-pert X-ray diffractometer (XRD) to determine the phases. Identification of the phases was achieved by comparing the sample diffractograms with the standard diffraction pattern cards from International Center for Diffraction Database (ICDD). EDX analyses were performed to check the chemical composition. Differential scanning calorimetry (DSC) was performed on porous and bulk NiTi to check transformation properties.

2.3 Ions release tests

Four samples of each material were completely immersed in 1 ml of cell culture media (see in “[In vitro cell culture analysis](#)” section) and maintained at 37 °C in 5 vol% CO₂ enriched air. At each time point (24, 48, 72 and 168 h) the media was extracted and diluted with 200 μ l of 37 % HCl (analytical grade, Sigma Aldrich) and deionized water up to 5 ml final volume. The use of chloridric environment

enhanced the solubility of titanium residual through complex formation.

To evaluate the release of Ni and Ti ions, the quantitative chemical analysis of these prepared solutions was carried out by inductively coupled plasma–optical emission spectroscopy (ICP–OES, Liberty 200, Varian, US). The analytical emission wavelengths were: Ni—231.604 nm; Ti—334.941 nm; the analytical detection limits for Ni and Ti were found to be 78 and 20 ppb respectively. For each schedule time, the samples were replicated four times and mean values were used to represent the concentrations.

2.4 In vitro cell culture analysis

MG63 Human Osteoblast-like cells purchased from Lonza (Italy) were cultured in Dulbecco Modified Eagle’s/F12 Medium (Gibco), containing penicillin/streptomycin (100 U/ml/100 μ g/ml) supplemented with 10 % fetal bovine serum and kept at 37 °C in an atmosphere of 5 % CO₂. Cells were detached from culture flasks by trypsinization and were centrifuged; cell number and viability were assessed with trypan-blue dye exclusion test. Each sample was washed in acetone for 10 min; EtOH 70 % for 20 min followed by three washes in PBS 1 \times for 10 min each. Samples were then air dried and sterilized by UV irradiation for 30 min under laminar flow hood. Samples were placed one per well in a 24-well plate and a drop of 50 μ l containing 1.25×10^3 cells (2.5×10^3 cells/cm²) was seeded on the centre of the upper sample surface allowing cell attachment for 40 min in the incubator, before addition into each well of 1.0 ml of cell culture medium. The medium was changed every 2 days. All cell-handling procedures were performed in a sterile laminar flow hood. All cell-culture incubation steps were performed at 37 °C with 5 % CO₂.

2.5 Cell viability assay

Live/Dead assay kit (Invitrogen) was performed according to manufacturer’s instructions. Briefly, the samples were washed with 1 \times PBS for 5 min and incubated with Calceinacetoxymethyl (Calcein AM) 2 μ M plus Ethidium homodimer-1 (EthD-1) 4 μ M for 15 min at 37 °C in the dark, the samples were rinsed in PBS 1 \times .

That assay is based on the simultaneous determination of live and dead cells with two probes, Calcein and EthD-1, that measure recognized parameters of cell viability: intracellular esterase activity and plasma membrane integrity respectively [20].

The live and dead cells ratio was determined by quantifying the number of cells in 3 fields at the same magnification for each sample after 24 and 48 h. Images were

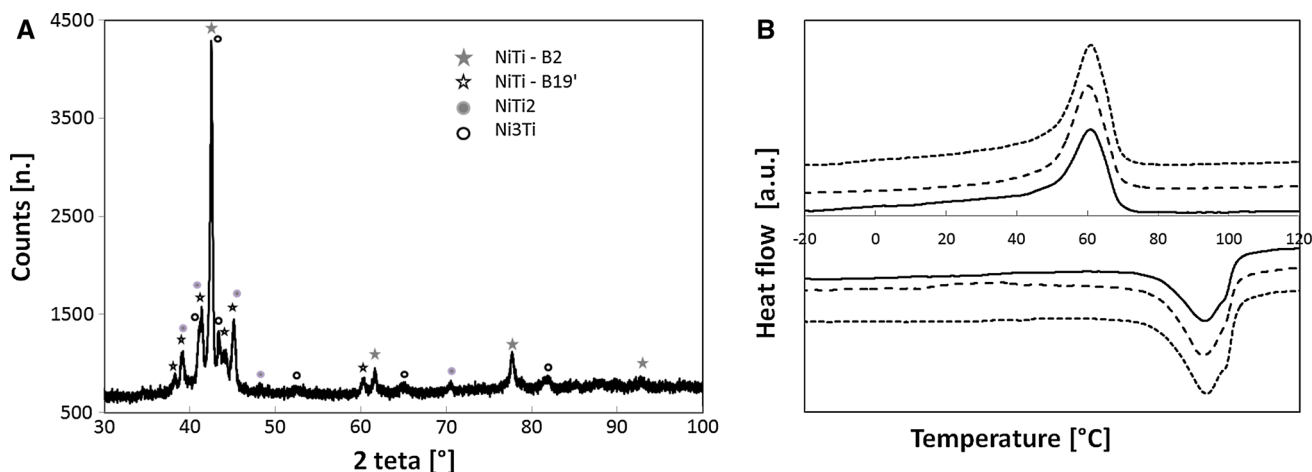


Fig. 2 Characterization of porous NiTi: **a** XRD analyses: NiTi phases of slightly different composition are present, together with NiTi₂ and Ni₃Ti phases. **b** Microstructure of the reacted sample is homogeneous as confirmed by DSC at three different position

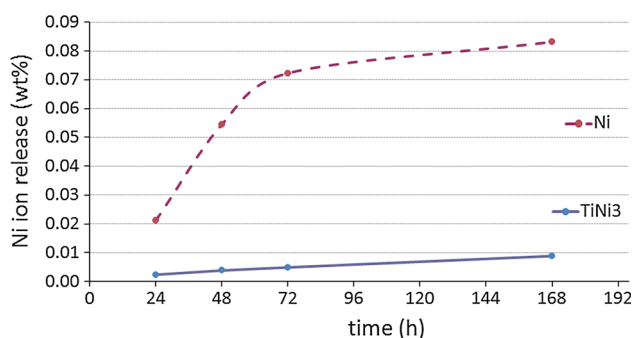


Fig. 3 Ni Ion release rate, for Ni and TiNi₃. For other material Ni content was below detection limits

acquired by an inverted Nikon Ti-E fluorescence microscope (Nikon). One sample per group was analysed.

2.6 Cell morphology evaluation

Two samples for each time point (24 and 48 h) were used for actin immunofluorescence and SEM analysis respectively. In order to visualize actin filaments samples were washed with PBS 1× for 5 min, fixed with 4 % (w/v) paraformaldehyde for 15 min and washed with PBS 1× for 5 min. Permeabilization was performed with PBS 1× with 0.1 % (v/v) Triton X-100 for 5 min. FITC-conjugated Phalloidin antibody (Invitrogen) 1:500 in PBS 1× was added for 20 min at room temperature in the dark [21].

Cells were washed with PBS 1× for 5 min and incubated with nuclear stain DAPI (Invitrogen) in PBS 1× for 5 min. The nuclear morphological changes in apoptotic cells were also evaluated. Apoptotic cells were identified by condensation of chromatin and/or nuclear fragmentation [22]. Images were acquired by an Inverted Ti-E fluorescence microscope (Nikon).

For scanning electron microscopy analysis, after 24 h one sample per group was washed with 0.1 M sodium cacodylate buffer pH 7.4 and fixed in 2.5 % glutaraldehyde in 0.1 M sodium cacodylate buffer pH 7.4 for 2 h at 4 °C, washed in 0.1 M sodium cacodylate buffer pH 7.4 and dehydrated in a graded series of ethanol for 10 min each. Dehydrated samples were sputter-coated with gold and observed using Stereoscan 360 Scanning Electron Microscope (Cambridge Instruments, UK).

2.7 Cell proliferation assay

MTT reagent (3-(4,5-dimethylthiazol-2-yl)-2,5-diphenyl-tetrazolium bromide) (Invitrogen) was prepared at 5 mg/ml in 1× PBS. N. 3 of bulk NiTi, porous NiTi, Ti₂Ni and Ti samples were incubated with the MTT reagent 1:10 for 2 h at 37 °C. Medium was collected and cells incubated with 1 ml of dimethyl sulfoxide for 15 min. In this assay, the metabolically active cells react with the tetrazolium salt in the MTT reagent to produce a formazan dye that can be observed at λ_{\max} of 570 nm, using a Multiskan FC Microplate Photometer (Thermo Scientific) [23].

This absorbance is directly proportional to the number of metabolically active cells. Mean values of absorbance were determined. Three samples per time point (24 h, 48 h, 72 h and 7 days) were analysed.

2.8 Statistical analysis

Results were expressed as mean \pm SEM plotted on graph. Analysis was made by two-way ANOVA, followed by Bonferroni's post hoc test. Statistical analysis was performed by the Graph Pad Prism software (version 5.0), with statistical significance set at $P \leq 0.05$.

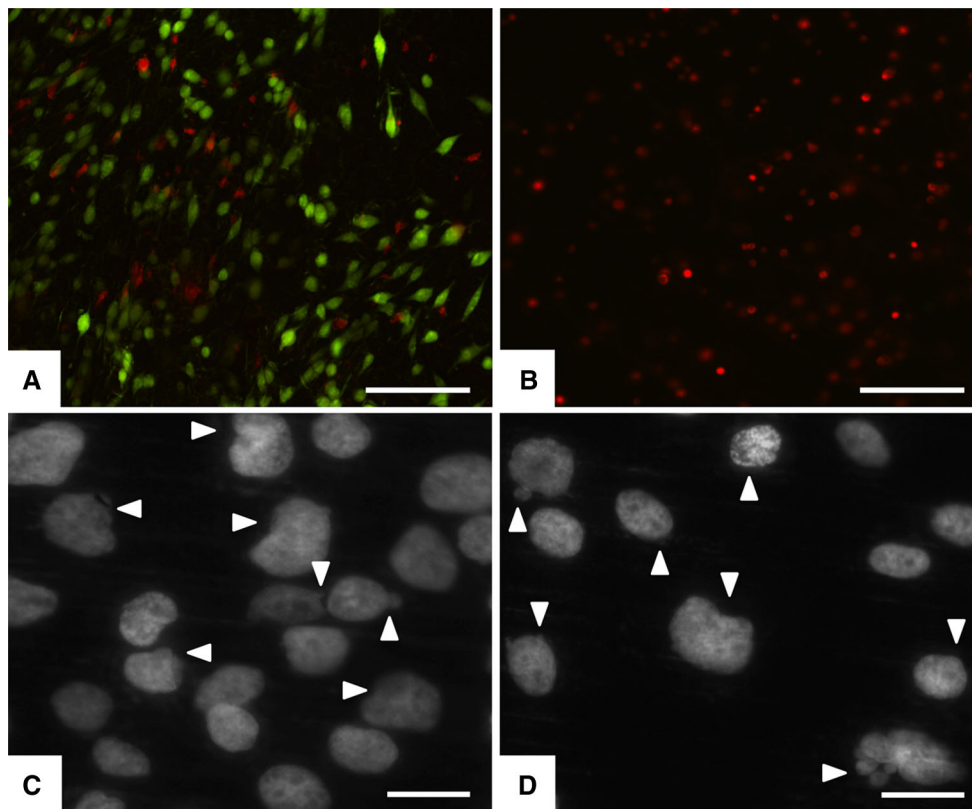


Fig. 4 Cell viability and nuclear morphological changes. Cell viability was analyzed by the Live/Dead assay. Calcein AM stains for live cells in green, EthD-1 stains for dead cells in red. Several dead cells were detected on sample TiNi₃ (a) and no live cells on Ni

sample (b) after 48 h of cells seeding. Apoptotic nuclei (indicated by the arrows) confirmed the low biocompatibility of samples TiNi₃ and Ni respectively (c and d). Scale bars a, b 100 μm and c, d 10 μm (Color figure online)

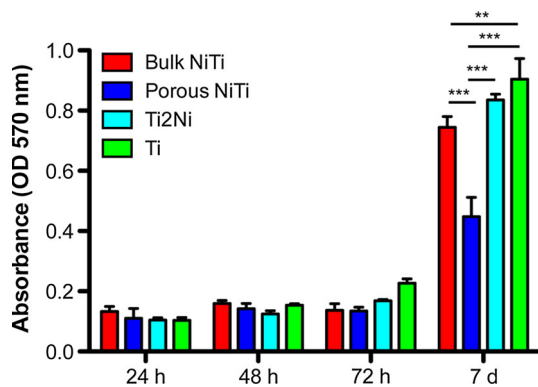


Fig. 5 Analysis of MG63 Human Osteoblast-like cells proliferation by the MTT assay, after 24 h, 48 h, 72 h, and 7 days. $^{**}P \leq 0.01$, $^{***}P \leq 0.001$, $n = 3$

3 Results and discussion

3.1 Microstructure and thermal analyses

As expected, XRD analyses of Ni, Ti, bulk NiTi, Ti₂Ni and TiNi₃ specimens showed only the patterns related to one

single phase. No additional peaks were found with respect to those listed in ICCD cards. While for porous NiTi specimens, produced by SHS, some low intensity peaks related to presence of Ti₂Ni and TiNi₃ as secondary phases were also detected. Local small differences of Ni content of NiTi phase [1] results in the presence, at room temperature, of both the two crystallographic structures of NiTi: austenite (cubic, B2) and martensite (monocline, B19') (Fig. 2a). The average phase content was similar all-over the reacted specimens: all DSC measurements provided similar results, as demonstrated in Fig. 2b. A measurement of secondary phase content was performed through image analysis of several backscattered electron images covering an area of 2 mm²: 1–3 % TiNi₃ and 3–6 % Ti₂Ni were estimated.

EDX analyses confirmed stoichiometric composition of the various phases, within the error limit of the technique (about ±0.2 a.t%).

3.2 Ions release tests

Chemical analyses of the solutions revealed that only TiNi₃ and Ni samples released detectable concentration of nickel

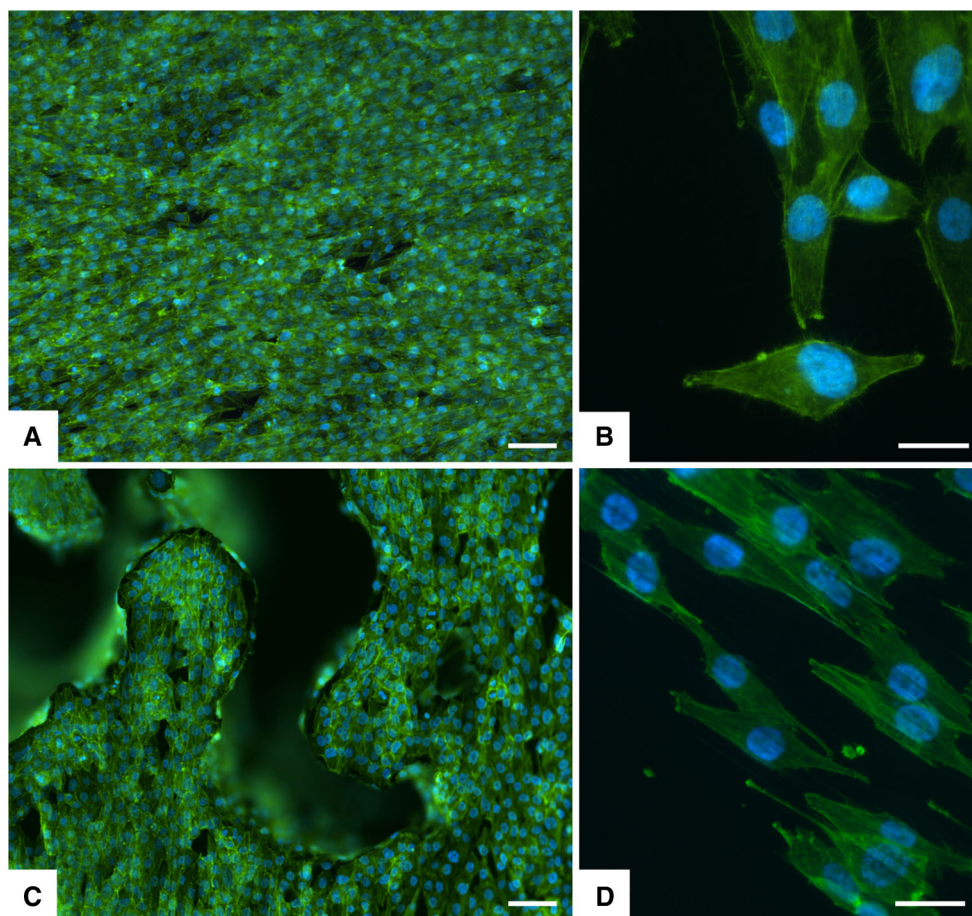


Fig. 6 Analysis of cell morphology by immunofluorescence images. Cells were spread with good morphology and firmly attached to the surface. After 48 h a cell layer covered the upper sample surface of bulk NiTi and porous NiTi respectively (**a** and **c**). Enlargement of

spread cells after 24 h of seeding on bulk NiTi and porous NiTi respectively (**b** and **d**). Phalloidin in *green* stains for actin filaments and DAPI in *blue* stains for cell nuclei. Scale bars **a**, **c** 100 μm and **b**, **d** 25 μm (Color figure online)

within 7 days. The measurements of nickel released from Ti_2Ni , Ti, bulk and porous NiTi samples and all the measurements of titanium were always lower than their detection limit.

In Fig. 3 the released mass percentages of nickel from TiNi_3 and Ni solutions as a function of immersion time are reported. The material with the highest amount of Ni (D sample, pure nickel), used as reference material, had a fastest degradation kinetic in physiological conditions. This sample exhibited a rapid release of nickel during the initial period of the immersion test (within 72 h); after further immersion time, very low increase of release rate was observed. Observed rates were within values reported in literature for bulk Ni exposed to artificial body fluid [24]. TiNi_3 sample continuously released nickel at a constant rate up to 7 days, but the total amount of ion dissolved (about 0.01 wt%) was about an eighth part of corresponding value for pure nickel (about 0.08 wt%).

The nickel released from the metallic samples increased as a function of nickel content, while this phenomenon did not occur in the case of titanium release, similarly to what observed by Bogdanski [8]. This effect occurred only when the amount of nickel was more than about 78 wt%, confirming that the latter value can be viewed as a threshold for the structural stability of Ti–Ni alloys.

The nickel ion release may be associated with the passivation effects related to the presence on titanium, for high titanium bearing alloys. Also a structure stoichiometry can be invoked to justify TiNi_3 behaviour: even if nickel content is only 25 % less than pure Ni, released nickel is far lower. It is worth to point out that among the three investigated intermetallics, TiNi_3 has the highest formation enthalpy.

Considering porous NiTi, it is generally reported to have higher release rate than bulk NiTi [5], due to increased active surface and presence of secondary phases. In our tests, possibly the porosity did not act as a channel for the

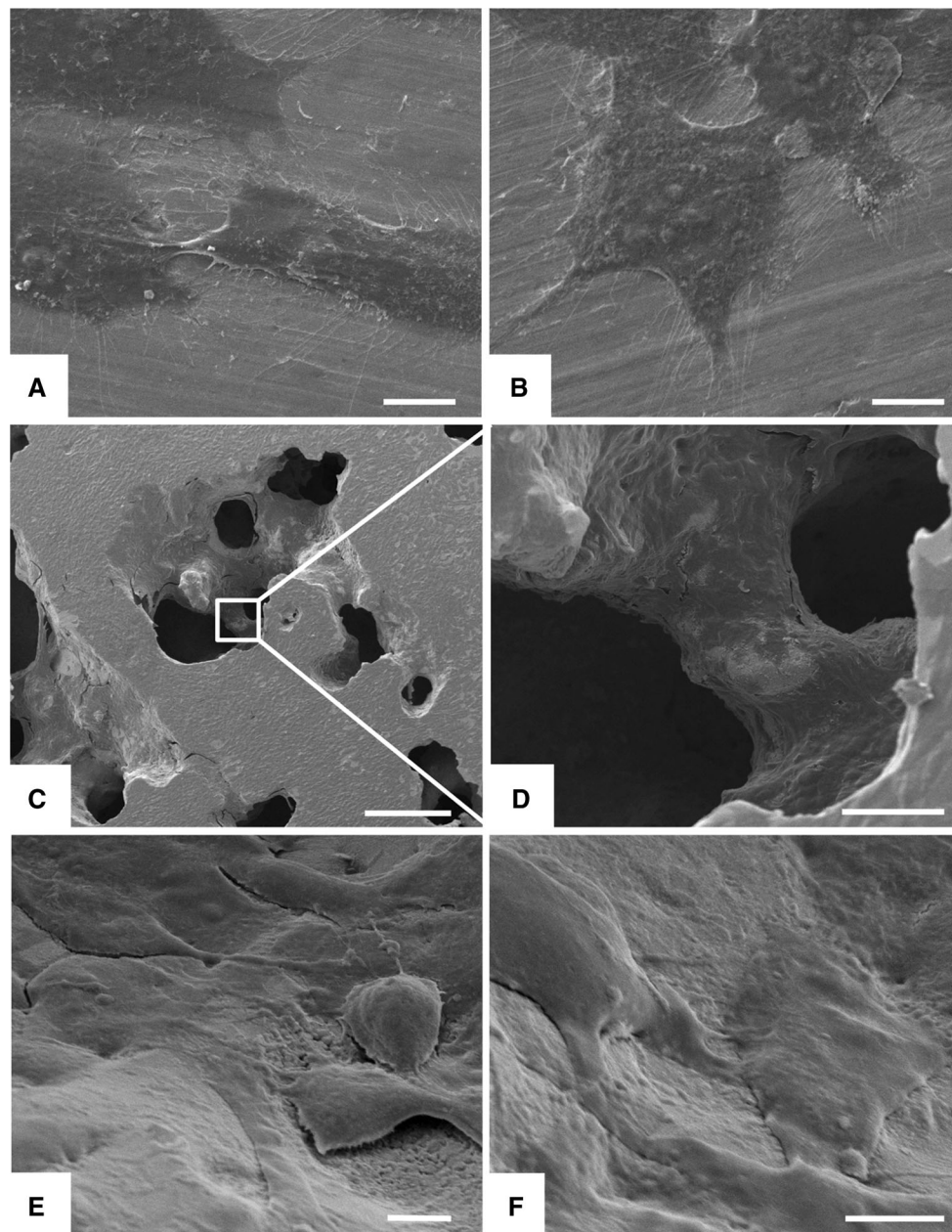


Fig. 7 Detailed analysis of cell morphology assessed by scanning electron microscopy. Attached cells on upper surface of bulk NiTi and porous NiTi samples respectively at 24 h (**a** and **b**). Low

magnification of porous NiTi sample (**c**) and detailed images of cells grown into its pores (**d**, **e**, **f**). Scale bars **a**, **b**, **e**, **f** 10 μm ; **c** 500 μm and **d** 100 μm

media, hence did not increase the metal ion release from the substrate. It is worth considering that even if an increased nickel released could have occurred, the total ion content was below detection limits.

3.3 In vitro cell analysis

Cell viability at 24 and 48 h were analysed by the Live/Dead assay. Results showed a very high ratio of viable cells at both experimental time points (approximately 99 %) on

bulk NiTi, porous NiTi, Ti_2Ni and Ti samples without any significant differences among the groups.

Live cells on sample TiNi_3 were very high at 24 h, but then decreased at 48 h with statistical differences with the other groups ($P \leq 0.001$) (Fig. 4a). No live cells were detected on Ni sample at both experimental time points (Fig. 4b). The nuclear morphological analysis showed high number of apoptotic cells seeded on TiNi_3 and Ni samples, confirming the low biocompatibility of these two samples (Fig. 4c, d).

Due to these results, the following *in vitro* investigations were done omitting TiNi₃ and Ni samples. Quantification of metabolically active cells was performed for each time point, by use of the MTT assay. Results demonstrated an increase in cell proliferation from day 1 to day 7 for all the samples (Fig. 5). The only statistically significant differences among the groups were identified at day 7. Porous NiTi sample showed a reduced cell proliferation compared to the other groups ($P \leq 0.001$). A possible reason for this fact could be its topography (Fig. 5). In fact, as confirmed by immunofluorescence and SEM morphological analysis, cells grown on porous NiTi samples had to change their morphology in order to adapt to the sample structure.

Cell–surface interaction and cell adhesion are complex processes involving the reorganization of cytoskeleton-proteins like actin [25]. Attachment phase of cell adhesion occurs rapidly and involves physicochemical linkages between cells and material. Cell spreading is an essential function of a cell which has adhered to a surface and precedes the function of cell proliferation to finally provide a cell covered surface as indicated in the Fig. 6. Analysis of phalloidin staining at 24 and 48 h after seeding did not reveal differences in cell morphology among the groups. Attached cells exhibited their characteristic intricate morphology and after 48 h cells covered almost the whole sample surface (Fig. 6). Another possible cause for reduced proliferation on porous NiTi is the presence of secondary phases in the material, especially of TiNi₃, and related Ni ion release, but this should be a minor cause, as no toxic Ni ion level was detected in the proliferation media.

Detailed cell morphology was analysed by scanning electron microscopy. After 24 h, cells were firmly attached to the samples surface, without any differences among the groups (Fig. 7) and after 48 h of culture; cells covered nearly the entire upper sample surface. Enlargements of the inner structure of porous NiTi sample, showed that after 24 h cells, seeded onto the upper surface, migrated through the interconnected porous structure and they were seen well attached to the inner surface (Fig. 7d–f).

4 Conclusions

Porous NiTi produced by SHS was characterised by the presence of NiTi phase and Ti₂Ni and TiNi₃ intermetallics. The comparison with bulk NiTi, Ti₂Ni, TiNi₃, pure Ni and Ti through the different biocompatibility tests allows to depict the following conclusions:

- Good biocompatibility of both NiTi with respect to Ti was observed

- Ti₂Ni revealed a biocompatibility close to or even better than NiTi: therefore it possibly doesn't decrease porous NiTi performances
- TiNi₃ was characterised by an appreciable nickel ion release rate, but lower with respect to what expected due to its high Ni content
- A slight difference between porous and bulk NiTi was observed during proliferation tests for the longest observation time. Topography can be considered the main reason for it, as it was verified that cells close to inner pores modified their structure in order to adapt to the new surface, hence reducing their reproduction capability.
- Further tests on specimen of porous NiTi with different topography and/or secondary phase content could help to further elucidate the observed phenomena.

Acknowledgments The authors acknowledge G. Carcano, P. Giuliani and E. Bassani for technical support.

References

1. Duerig T, Pelton A, Stockel. An overview of nitinol medical applications. *Mater Sci Eng A Struct* 1999; 273:149.
2. Elahinia M, Hashemi M, Tabesh M. Manufacturing and processing of NiTi implants: a review. *Prog Mater Sci.* 2012;57:911.
3. Greiner C, Oppenheimer SM, Dunand DC. High strength, low stiffness, porous NiTi with superelastic properties. *Acta Biomater.* 2005;1:705.
4. Alvarez K, Nakajima H. Metallic scaffold for bone regeneration. *Materials.* 2009;2:790.
5. Bansiddhi A, Sargeant TD, Stupp SI, Dunand DC. Porous NiTi for bone implants: a review. *Acta Biomater.* 2008;4:773.
6. Ou M, Watari F, Yokoama A, Matsuno H, Kawasaki T. Dissolution of nickel and tissue response observed by X-ray scanning analytical microscope. *Biomaterials.* 1999;20:747.
7. Es-Souni M, Es-Souni M, Fischer-Brandies H. Assessing the biocompatibility of NiTi shape memory alloys used for biomedical applications. *Anal Bioanal Chem.* 2005;381:557.
8. Bogdanski D, Koeller M, Mueller D, Muhr G, Bram M, Buchkremer HP, Stoeber D, Choi D, Epple M. Easy assessment of the biocompatibility of NiTi alloys by *in vitro* cell culture experiments on a functionally graded Ni-NiTi-Ti material. *Biomaterials.* 2002;23:4549.
9. Vandekerckhove R, Chandrasekaran M, Vermaut P, Portier R, Delaey L. Corrosion behaviour of a superelastic Ni–Ti alloy. *Mater Sci Eng A Struct* 2004; 378:532.
10. Shabalovskaya S, Shabalovskaya S, Van Humbeeck J. Critical overview of Nitinol surfaces and their modifications for medical applications. *Acta Biomater.* 2008;4:447.
11. Shabalovskaya S, Anderegg J, Van Humbeeck J. Recent observations of particulates in Nitinol. *Mater Sci Eng A Struct* 2008; 481:431.
12. Wever DJ, Veldhuizen AG, de Vries J, Busscher HJ, Uges DRA, van Horn JR. Cytotoxic, allergic and genotoxic activity of a nickel–titanium alloy. *Biomaterials.* 1997;18:1115.
13. Thierry B, Tabrizian M, Trépanier C, Savadogo O, Yahia LH. Effect of surface treatments and sterilization processes on the

- corrosion behavior of NiTi shape memory alloy. *J Biomed Mater Res.* 2000;51:685.
14. Rondelli G, Vicentini B, Cigada A. The corrosion behaviour of nickel titanium shape memory alloys. *Corros Sci.* 1990;30(8/9):805.
 15. Shabalovskaya S, Andereg J, Rondelli G, Vanderlinden W, De Feyter S. Comparative in vitro performances of bare Nitinol surfaces. *Bio Med Mater Eng.* 2008;18:1.
 16. Zhao Y, Taya M, Kang Y, Kawasaki A. Compression behavior of porous NiTi shape memory alloy. *Acta Mater.* 2005;53:337.
 17. Kaya M, Bugutekin A, Orhan N. Effect of solution treatment on thermal conductivity of porous NiTi shape memory alloy. *Int J Thermophys.* 2011;32:665.
 18. Biswas A. Porous NiTi by thermal explosion mode of SHS: processing, mechanism and generation of single phase microstructure. *Acta Mater.* 2005;53:1415.
 19. Zanotti C, Giuliani P, Bassani P, Zhang Z, Chrysanthou A. Comparison between the thermal properties of fully dense and porous NiTi SMAs. *Intermetallics.* 2010;18:14.
 20. Papadopoulos NG, Dedoussis GV, Spanakos G, Gritzapis AD, Baxevanis CN, Papamichail M. An improved fluorescence assay for the determination of lymphocyte-mediated cytotoxicity using flow cytometry. *J Immunol Methods.* 1994;177:101.
 21. Faulstich H, Zobeley S, Rinnerthaler G, Small JV. Fluorescent phallotoxins as probes for filamentous actin. *J Muscle Res Cell Motil.* 1988;5:370.
 22. Plotkin L, Weinstein RS, Parfitt AM, Roberson PK, Manolagas SC, Bellido T. Prevention of osteocyte and osteoblast apoptosis by bisphosphonates and calcitonin. *J Clin Invest.* 1999;104:1363.
 23. Liu Y, Peterson DA, Kimura H, Schubert D. Mechanism of cellular 3-(4,5-dimethylthiazol-2-yl)-2,5-diphenyltetrazolium bromide (MTT) reduction. *J Neurochem.* 1997;69:581.
 24. Mazinianian N, Hedberg Y, Wallinder IO. Nickel release and surface characteristics of fine powders of nickel metal and nickel oxide in media of relevance for inhalation and dermal contact. *Regul Toxicol Pharm* 2013;65:135.
 25. Anselme K. Osteoblast adhesion on biomaterials. *Biomaterials.* 2002;21:667.